NANO LETTERS

2004
Vol. 4, No. 12
2383−2387

Finite-Size Effect and Wall Polarization in a Carbon Nanotube Channel

Deyu Lu, Yan Li, Slava V. Rotkin,† Umberto Ravaioli, and Klaus Schulten*

Beckman Institute for Advanced Science and Technology, University of Illinois at Urbana Champaign, 405 N. Mathews, Urbana, Illinois 61801

Received September 4, 2004; Revised Manuscript Received October 7, 2004

ABSTRACT

The electronic structure and dielectric screening of finite-length armchair carbon nanotubes are studied in view of their technical applications. For this purpose, a self-consistent tight-binding method, which captures the periodic oscillation pattern of the finite band gap as a function of tube length, is applied. We find the parallel screening constant $\epsilon_{\parallel}$ to grow nearly linearly with the length L and to show little dependence on the band gap. In contrast, the perpendicular screening constant $\epsilon_{\perp}$ is strongly related to the band gap and converges for $L > 10R$ (radius) to its bulk value. Our description is employed to study the wall polarization in a short (6,6) nanotube filled with six water molecules, a situation that arises with technical uses of carbon nanotubes as channels.

Single-walled carbon nanotubes (SWNTs) can be classified as metallic, quasi-metallic, or semiconducting, depending on how they are wrapped up from graphene layers.[1] When SWNTs are shortened, their energy levels become quantized, which makes them suitable for applications such as quantum dots and single-electron transistors.[2] It has also been proposed that the small size and stable structure make short SWNTs good candidates for artificial nanoscale channels for transport of water,[3−6] protons,[7,8] ions,[9] or polymers.[10] Recent experiments using X-ray diffraction[11] and neutron scattering[12] provided insight into the properties of nanotube-confined water. The observations revealed a chain of water molecules wrapped by a shell of water, all encapsulated inside SWNTs with diameter around 1.4 nm.[12] These experiments confirm an earlier prediction that water can enter the hydrophobic interior of narrow SWNTs.[3−6]

From the modeling point of view, artificial SWNT channels have been studied by means of molecular dynamics (MD) simulations, focusing on both filling and transport properties.[3−6] In the previous simulations, the interaction between water and the SWNT was usually treated through a short-range van der Waals potential, and little attention was paid to the polarizable nature of the SWNT. Unlike many biological channels, SWNTs are highly polarizable due to their delocalized π-electrons, which respond strongly to external fields. A study of screening effects of infinitely long SWNTs to an external point charge impurity has revealed that metallic nanotubes can effectively screen out the long-range Coulomb potential along the axial direction, while screening effects in semiconducting tubes are weaker.[13] Neglecting the polarization of SWNTs could be misleading because the filling and transport properties of water are sensitive to the water−SWNT interaction.[3] Therefore, knowledge of the dielectric response of finite-size SWNTs is essential for an understanding of water/ion/polymer permeation and for designing efficient SWNT channels.

In recent studies,[7,8] density functional theory (DFT) calculations have been carried out in MD simulations to take into account the electronic degrees of freedom. However, the finite-size effect on the dielectric response is not well characterized in these studies, and further applications are prohibited by the high computational cost. In this work, we used a self-consistent tight-binding (TB) method to study the electronic properties of finite-length armchair nanotubes and observed how the screening behavior evolves from 0D to 1D as the tube length increases. We believe that our method can be efficiently combined with MD simulations to investigate nanotube-based channels.

An infinitely long armchair nanotube is metallic, but a HOMO (highest occupied molecular orbital)/LUMO (lowest unoccupied molecular orbital) gap opens in finite-length tubes. First principle results from different groups[2,14,15] agree in that the gap oscillates as a function of tube length with a period of three sections. Interestingly, the obtained gap minima are nonzero, contrary to the prediction from TB theory with only nearest neighbor interactions.

In the following we show that the period of oscillation can be explained by imposing the quantum box boundary condition and that the nonzero band gap minima can be reproduced by including third-nearest-neighbor (NN) interactions. For armchair SWNT segments with ideal geometry,

* Corresponding author. E-mail: kschulte@ks.uiuc.edu.
† Present address: Department of Physics, Lehigh University, 16 Memorial Drive East, Bethlehem, PA 18015.

10.1021/nl0485511 CCC: $27.50
Published on Web 10/26/2004

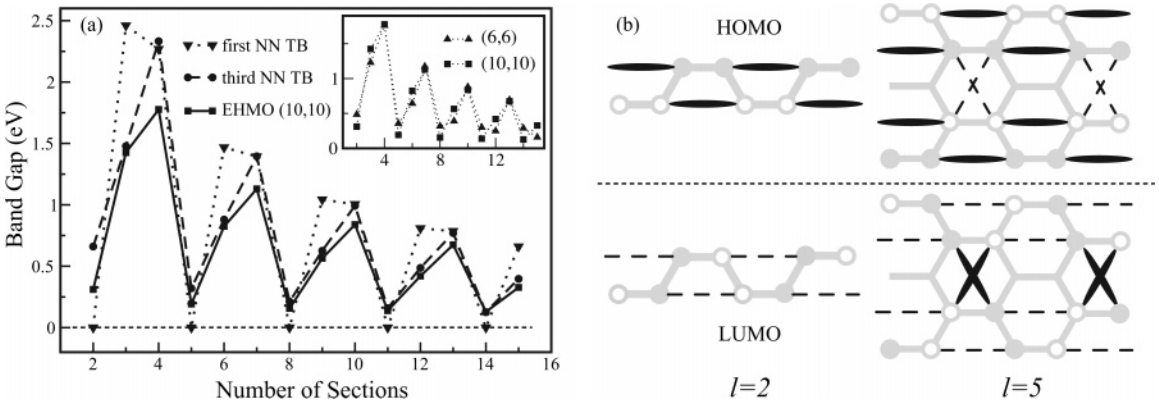

Figure 1. (a) Band gap variation of a (10,10) nanotube as a function of tube length. EHMO band gaps of a (6,6) and a (10,10) nanotube are compared in the inset to demonstrate the curvature effect. (b) Schematic description of the HOMO and LUMO orbitals of armchair nanotubes with 2 (left) and 5 (right) sections. The positive and negative phases of the wave function are denoted by solid and open circles, whose size represents the magnitude of the phase. A bonding or antibonding state is characterized by a dark oval or a broken line.

it has been demonstrated that HOMO/LUMO gaps calculated from the extended Hückel model (EHMO)[16] are close to those from DFT.[2] Therefore, we use the EHMO to test our TB model. The first-, second-, and third-NN hopping integrals used in our study are $\gamma_0 = -2.97$ eV, $\gamma_1 = -0.073$eV, $\gamma_2 = -0.33$ eV,[17] respectively, and the overlap integrals are neglected. For the sake of simplicity, the structure optimization effect[14,15] is neglected, which can be incorporated later by adopting distance-dependent hopping integrals.

Consider an armchair SWNT aligned along the z direction. The electronic states of the nanotube are characterized by the angular momentum quantum number m in the x-y plane and the axial wave vector k. The quantum box boundary condition selects the quantized wave vectors $k = p\pi/L$, where $p = 1, 2, 3, \cdots$; $L = (l + 1)a/2$ is the length of the nanotube segment with $a = 2.46$ Å being the lattice constant and l the number of sections. It is convenient to write $k = 3pk_F/(l + 1)$, where $k_F = 2\pi/3a$ is the wave vector at the Fermi point. Segments of all possible lengths can be categorized into three subclasses characterized by $l = 3s + j$, where $j = 0, \pm 1$ and s is a positive integer. Let $|k - k_F|$ be minimized at k_{min}. The offsets, $\Delta k \equiv k_{min} - k_F$, take values 0, $-k_F/(3s + 1)$, and $k_F/(3s + 2)$ at $j = -1$, 0, 1, respectively. The band gap is determined by the linear dispersion relationship near k_F, $E_g = 2v_F|\Delta k|$, where $v_F = (\sqrt{3}/2)\gamma_0 a$ is the Fermi velocity.[1] It follows directly that the band gap oscillates with a period of 3 in l. The tube length dependence of the band gap from TB and EHMO is compared in Figure 1a. As one can see from both the nearest neighbor TB model and EHMO, the band gap oscillates with a period of 3. Similarly, within each period, there is a minimum at $j = -1$. However, the NN TB model does not reproduce the finite band gap in EHMO, yielding a zero band gap instead for $j = -1$. This discrepancy could be detrimental for a proper description of polarizabilities.

The discrepancy can be understood as follows. Within the first-NN TB Hamiltonian, the HOMO and LUMO orbitals, $|\pi\rangle$ and $|\pi^*\rangle$, can be constructed from the linear combination of $|\pi_A\rangle$ and $|\pi_B\rangle$, the degenerate standing wave states at k_{min} of sublattices A and B of the SWNT. k_{min} coincides with k_F at $j = -1$, thus $|\pi_A\rangle$ and $|\pi_B\rangle$ become eigenstates, which implies that $|\pi\rangle$, $|\pi^*\rangle$ are also degenerate and, hence, the band gap vanishes. The second-NN interaction, γ_1, involves atoms of the same sublattice, so it only shifts the on-site energy of A and B by the same amount but does not eliminate the degeneracy. To lift the degeneracy, one needs to include also the third-NN interaction, γ_2. The HOMO and LUMO states are depicted in Figure 1b for $l = 2$ and $l = 5$. An atom and its third-NN form a bonding state if their π-orbitals are parallel; they form an antibonding state if the π-orbitals are antiparallel. Due to the finite length of the nanotube, HOMO (LUMO) has more (less) bonding states than antibonding states. The gap minima at $j = -1$ are described by

$$E_g^{min} = -2\gamma_2/s \tag{1}$$

The HOMO/LUMO gap decreases as a nanotube becomes longer and vanishes at infinite length, consistent with the continuum model. Band gaps from the third-NN TB model are also plotted in Figure 1a, successfully reproducing the oscillation pattern and capturing well the gap minima. It is also found that for (n,n) nanotubes with $n \geq 8$, the HOMO and LUMO orbitals obtained in our third-NN TB model are nearly identical to those from EHMO.

When the tube becomes narrower, effects due to curvature emerge. The EHMO band gap patterns of (6,6) and (10,10) nanotubes are compared in the inset of Figure 1a (same as Figure 5 in ref 2). While the maxima of the (6,6) tube are still at $j = 1$, the minima change from $j = -1$ to $j = 0$ when $s \geq 4$. The change in gap minima results from a shift of the real Fermi point from k_F to k'_F due to the curvature effect.[18] For armchair nanotubes, it can be proved that the relationship holds

$$\Delta k_F \equiv k'_F - k_F = -\frac{\pi}{2\sqrt{3}n^2}k_F \tag{2}$$

As Δk_F is negative and assuming Δk_F is small compared to π/L, one concludes that the band gap increases at $j = -1$, and decreases by the same amount at $j = 0$. Without

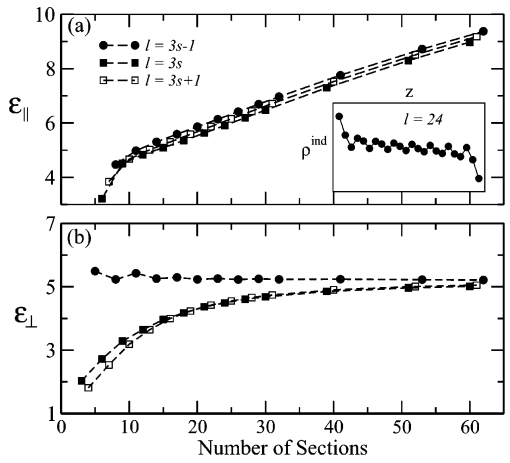

Figure 2. Dielectric screening constant in the direction (a) parallel or (b) perpendicular to the tube axis for a (10,10) SWNT as a function of the number of sections l. The inset shows the corresponding induced charge distribution at $l = 24$ along the axis (summed over the circumference).

considering the curvature effect, the band gap difference between subclasses $j = -1$ and $j = 0$ diminishes as l gets larger. Whenever this difference becomes smaller than $2v_F|\Delta k_F|$, the minima of the band gap switch to $j = 0$ as seen in the inset of Figure 1a.

The dielectric properties of SWNTs can be characterized by defining a dielectric constant $\epsilon = V_{ext}/V_{tot}$, relating the external and total electrostatic potential V_{ext} and V_{tot} defined on the SWNT surface. In Fourier space, the dielectric function can be written as $\epsilon_m(q) = 1 + \chi_m(q)G_m(q)$, where the density response function $\chi_m(q)$ and the electrostatic kernel $G_m(q)$ are labeled by the axial wave vector q and angular quantum number $m \equiv k_\theta R$. The electric potentials imposed by uniform electric fields parallel and perpendicular to the axis correspond to $m = 0$, $q \rightarrow 0$, and $m = \pm 1$, $q = 0$, respectively.[19] To investigate the size effect on the dielectric behavior of SWNTs, we extract the average screening constant $\epsilon_{||}$ and $\epsilon_\perp$ at the middle region of a short SWNT and compare the results with those for long SWNTs.

Parallel Dielectric Response. The parallel dielectric function $\epsilon_{||}(q)$ depends on the type of SWNT; e.g., in the long wavelength limit $\chi_0(q)$ is a constant for metallic SWNTs and $\chi_0(q) \propto q^2$ for semiconducting SWNTs.[20] In contrast to bulk materials where $G(q) \propto q^{-2}$, for quasi-1D materials such as nanotubes, $G_0(q)$ diverges as $\ln(qR)$. Thus, an infinitely long armchair nanotube is predicted to completely screen out parallel electric fields,[19] since $\lim_{q\rightarrow 0} \epsilon_{||}^{met}(q) \propto \lim_{q\rightarrow 0} -\ln(qR) \rightarrow \infty$. However, since the screening mostly arises from contributions at small q's through $\ln(qR)$, by limiting the length of the SWNTs, we expect a drastic reduction of their screening ability, as $q_{min} \sim 1/L$. In Figure 2a, we plot the length dependence of $\epsilon_{||}$ for a (10,10) SWNT calculated by the self-consistent TB method. Here, $\epsilon_{||}$ increases almost linearly with the tube length and the three subclasses of l collapse almost independent of their band gaps, which may differ by a factor of 4 to 5. This seems to be in contrast to the case of infinitely long semiconducting SWNTs, where $\epsilon_{||} \sim E_g^{-2}$.[19] In this case, the independence of the HOMO/LUMO band gap comes from the specific symmetry of armchair SWNTs, which forbids the direct transition from the HOMO state to the LUMO state due to their opposite parities about the vertical mirror operation.[21] Only transitions between states with the same parities are allowed, and due to energy quantization, the lowest transition energy scales as $\Delta E \sim 1/l$. One also finds that at fixed length L, the dielectric response becomes stronger as the radius of the nanotube decreases, as a result of the increasing aspect ratio L/R.

Shown in the inset of Figure 2a is the induced charge distribution ρ^{ind} on a (10,10) SWNT with 24 sections. In the middle region, ρ^{ind} is almost linearly distributed, while a larger portion of positive and negative charges accumulates at the ends due to the edge effect. In addition to the linear profile, the induced charges also oscillate along the axis with a wavelength of $\lambda = 3a/2$, corresponding to the length of three sections. This can be understood from the energy spectrum of an infinitely long armchair SWNT, which has degenerate states at the two Fermi points $\pm k_F$. Transition between these two energetically equivalent states results in an infinite response function $\chi(q)$ at $q = 2k_F = 2\pi/\lambda$, which causes the short wavelength Friedel oscillation of ρ^{ind}.[13] This type of oscillation is largely independent of models and was seen in earlier calculations.[22]

Perpendicular Dielectric Response. It is predicted that for infinitely long SWNTs the perpendicular dielectric constant $\epsilon_\perp$ is about 5, almost independent of the radius.[19,21] Figure 2b shows the length dependence of $\epsilon_\perp$, which is always larger for $l = 3s - 1$, compared to the other two subclasses. In this case, due to the conservation of angular momentum, only coupling between states with $\Delta m = \pm 1$ is allowed.[21] A smaller band gap corresponds to a smaller transition energy and results in a larger dielectric constant. Unlike the parallel dielectric response, $\epsilon_\perp$ quickly converges to its bulk value when the length exceeds a value 10 times the radius. This is due to $\lim_{q\rightarrow 0} G_{\pm 1}(q) \rightarrow$ constant, leaving the long wavelength contribution less important than in the parallel case. A small increase in $\epsilon_\perp$ is observed when the nanotube becomes narrower.

Dipole Screening. Figure 3 depicts the dielectric response of a short (6,6) SWNT to an external dipole μ_0, consisting of two unit charges of opposite sign separated by a distance $a/2$ along the tube axis. μ_0 is effectively screened by the induced charges ρ^{ind} on the SWNT when positioned near the SWNT center ($z = 0$), with the ratio $|\mu^{tot}/\mu_0| < 15\%$ for $l \geq 12$, where $\mu^{tot} = \mu_0 + \sum_i \rho_i^{ind} z_i$. The ratio approaches 1 as the external dipole μ_0 moves toward the tube edge until the induced dipole flips its sign when μ_0 moves outside and imposes an effective attraction to the external dipole. This feature may affect the entering probability of dipole molecules, e.g., water, into the SWNT channel.

Figure 4 is a snapshot taken from a classical MD simulation with the same parameters as used recently.[6] The simulated (6,6) nanotube is 13.4 Å long and 8.2 Å in diameter. Due to the confinement of the tube interior, six water molecules are arranged in single file. By forming hydrogen bonds, their dipole moments are preferably aligned

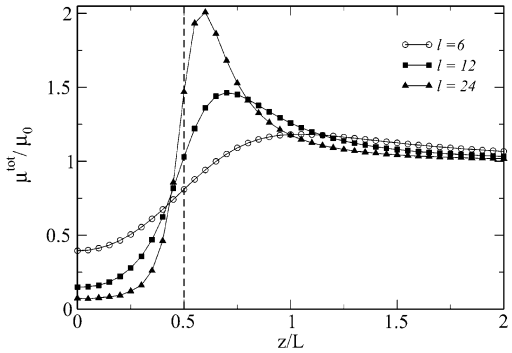

Figure 3. Effective screening ratio μ^{tot}/μ_0 of a dipole positioned along the axis of a (6,6) SWNT. The location of the dipole relative to the tube center z is scaled by tube length L with 6, 12, 24 sections, respectively. The dashed line indicates the right end of the finite SWNT.

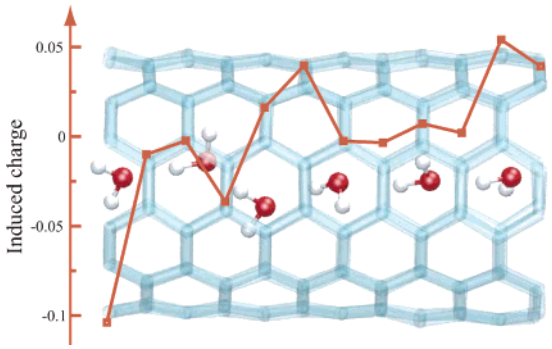

Figure 4. Background is a snapshot taken from a MD simulation of a 6-water-wire (ball-stick representation) inside a (6,6) nanotube segment with 12 sections. Water molecules outside the nanotube are not shown for clarity. The overlaying curve plots the summed induced surface charges (in squares) of each section of the nanotube. This figure was produced with VMD.[25]

along the tube axis. During the 1 ns simulation, the total dipole moment of the confined water molecules is 13.48 ± 1.28 Debye, with an axial component of −11.57 ± 1.31 Debye. For the given snapshot, the total water dipole is 12.23 Debye. The electrostatic field of the water dipoles polarizes the nanotube and induces a charge distribution on the nanotube surface (see Figure 4). The resulting effective counter-dipole leads to a net dipole of 5.24 Debye, which is much less than the original value. A similar strong screening effect has also been observed in an ab initio calculation.[8]

The polarization of SWNTs is expected to affect the filling of nanotubes. According to previous classical MD studies, filling of the hydrophobic (6,6) SWNT interior results from a delicate energy balance, which is subject to change under external perturbations as small as a few k_BT.[3] Provided that the Coulomb energy between the confined water wire and the image charges on the SWNT is about 6 k_BT, the polarization effect is indeed not negligible, and the filled state is expected to be energetically more favorable than the unfilled state. The polarization effect also plays a key role in proton transport through a water-filled SWNT. Compared with a neutral water wire, the energy of the water−SWNT complex is lowered when a proton is introduced at the middle of the water wire. This enhanced stabilization is mainly due to the interaction between the proton and its image charge. The stabilization energy can be roughly estimated as −0.66 eV by considering a single positive charge at the center of the nanotube in our model, which agrees with the −0.60 eV value from ab initio calculation.[8] On the other hand, it has been proposed to functionalize short SWNTs or apply external electric fields to enhance the transport of water and/or ions.[6,9] In these situations, the screening from the surface charges on the SWNT is also important. Another factor that could affect molecular transport is the edge effect. For SWNTs saturated with hydrogen atoms at edges, DFT calculations[23] reveal a significant charge transfer between the hydrogen and carbon atoms at zero external field. This charge redistribution contributes significantly to the electric field near the tube edges.

For the model system discussed above, six water molecules confined in a short SWNT, full quantum mechanical simulations are tractable today. However, approximate yet qualitatively correct quantum mechanics/molecular mechanics methods need to be developed to properly characterize the polarizability of SWNTs for even larger systems. For example, to simulate nucleic acid transport through a carbon nanotube channel as observed recently,[24] one needs to account for ions, several base pairs of DNA, more than one thousand carbon atoms from the nanotube, and several thousand water molecules in the unit cell. In this case, full quantum mechanical calculations are too formidable, but the scheme proposed here is very suitable. Work is in process to study the molecular transport in short polarizable SWNTs by combining MD simulation[6] with our computational scheme.

We have studied the electronic structure of finite-length armchair SWNTs within a TB description. By including the third-nearest-neighbor interactions, we reproduce successfully the DFT oscillation pattern of the band gap as a function of tube length. As the tube length increases, the three subclasses of SWNTs exhibit similar responses for parallel fields and different responses for perpendicular fields. The polarization effect of short SWNTs was also illustrated by computing the induced charges of a water-filled SWNT. Substantial screening of the dipole moment of the confined water molecules is found and the Coulomb interaction energy between water and the image charges (about 6 k_BT) turns out to be appreciable. The proper modeling of carbon nanotube wall polarization provided by our method even for large systems should advance further studies of molecular transport through carbon nanotube channels.

Acknowledgment. This work was supported by NSF grants CCR 02-10843, CCR 01-21616, MCB 02-34938, and EEC-0228390, by NIH grant P41-RR05969, by the ARMY DURINT contract SIT 527826-08, and by DoE grant DE-FG02-01ER45932.

References

(1) Saito, R.; Dresselhaus, G.; Dresselhaus, M. S. *Physical Properties of Carbon Nanotubes*; Imperial College Press: Singapore, 1998.
(2) Rochefort, A.; Salahub, D. R.; Avouris, Ph. *J. Phys. Chem. B* **1999**, *103*, 641−646.

(3) Hummer, G.; Rasaiah, J. C.; Noworyta, J. P. *Nature* **2001**, *414*, 188−190.
(4) Noon, W. H.; Ausman, K. D.; Smalley, R. E.; Ma, J. *Chem. Phys. Lett.* **2002**, *355*, 445−448.
(5) Mashl, R. J.; Joseph, S.; Aluru, N. R.; Jakobsson, E. *Nano Lett.* **2003**, *3*, 589−592.
(6) Zhu, F.; Schulten, K. *Biophys. J.* **2003**, *85*, 236−244.
(7) Dellago, C.; Naor, M. M.; Hummer, G. *Phys. Rev. Lett.* **2003**, *90*, 105902−105905.
(8) Mann, D. J.; Halls, M. D. *Phys. Rev. Lett.* **2003**, *90*, 195503−195506.
(9) Joseph, S.; Mashl, R. J.; Jakobsson, E.; Aluru, N. R. *Nano Lett.* **2003**, *3*, 1399−1403.
(10) Wei, C.; Srivastava, D. *Phys. Rev. Lett.* **2003**, *91*, 235901−235904.
(11) Maniwa, Y.; Kataura, H.; Abe, M.; Suzuki, S.; Achiba, Y.; Kira, H.; Matsuda, K. *J. Phys. Soc. Jpn.* **2002**, *71*, 2863−2866.
(12) Kolesnikov, A. I.; Zanotti, J.-M.; Loong, C.-K.; Thiyagarajan, P.; Moravsky, A. P.; Loutfy, R. O.; Burnham, C. J. *Phys. Rev. Lett.* **2004**, *93*, 035503.
(13) Lin, M. F.; Chuu, D. S. *Phys. Rev. B* **1997**, *56*, 4996−5002.
(14) Cioslowski, J.; Rao, N.; Moncrieff, D. *J. Am. Chem. Soc.* **2002**, *124*, 8485−8489.
(15) Matsuo, Y.; Tahara, K.; Nakamura, E. *Org. Lett.* **2003**, *5*, 3181−3184.
(16) Landrum, G. *YAeHMOP (Yet Another Extended Hückle Molecular Orbital Package)*; Cornell University: Ithaca, New York, 1995.
(17) Reich, S.; Maultzsch, J.; Thomsen, C.; Ordejón, P. *Phys. Rev. B* **2002**, *66*, 035412−035416.
(18) Kleiner, A.; Eggert, S. *Phys. Rev. B* **2001**, *64*, 113402−113405.
(19) Benedict, L. X.; Louie, S. G.; Cohen, M. L. *Phys. Rev. B* **1995**, *52*, 8541−8549.
(20) Léonard, F.; Tersoff, J. *Appl. Phys. Lett* **2002**, *81*, 4835−4837.
(21) Li, Y.; Rotkin, S. V.; Ravaioli, U. *Nano Lett.* **2003**, *3*, 183−187.
(22) Bulashevich, K. A.; Rotkin, S. V. *JETP Lett.* **2002**, *75*, 205−209.
(23) Lu, D.; Li, Y.; Ravaioli, U.; Schulten, K., unpublished.
(24) Ito, T.; Sun, L.; Crooks, R. M. *Chem. Commun.* **2003**, 1482−1483.
(25) Humphrey, W.; Dalke, A.; Schulten, K. *J. Mol. Graph.* **1996**, *14*, 33−38.

NL0485511